Journal of the Korean Physical Society, Vol. 41, No. 2, August 2002, pp. 212∼220

# High-Recycling Characteristics in the KSTAR Tokamak Divertor by Using Two-Dimensional Transport Simulations

Jin-Seok Ko,* Deok-Kyu Kim and Sang Hee Hong
*Department of Nuclear Engineering, Seoul National University, Seoul 151-742*

Ki-Hak Im
*Korea Basic Science Institute, Daejeon 305-333*

(Received 8 March 2002)

The operation space in the conduction-limited divertor regime of the KSTAR (Korea Superconducting Tokamak Advanced Research) tokamak is obtained in terms of the upstream density and the input power through numerical simulations using a two-dimensional two-fluid edge plasma transport code coupled with a two-dimensional Monte Carlo recycling neutral transport code in which the electron impact ionization and the charge exchange of recycling neutrals are taken into account. Two major high-recycling characteristics, the parallel temperature gradient and plasma pressure conservation, are identified in this operation space along the magnetic flux tubes between the upstream position and the divertor target plate in the KSTAR tokamak. Inclusion of ion pressures in the present simulations for total plasma pressures shows firm evidence of pressure conservation in the high-recycling regime. In addition, scalings of the plasma temperature and density at the divertor plate with the upstream plasma density are derived, and they are compared with those in a simple one-dimensional analytic transport model, the so-called two-point model. Finally, the simulation shows that the peaked feature of the upstream ion temperature profile adjacent to the separatrix affects the distribution of the divertor heat flux. This indicates that the ion parallel heat conduction near the separatrix plays an important role in determining the radial profile of the heat flux onto the divertor target, as the electron parallel heat conduction does in the conduction-limited regime. It is, therefore, suggested that modification of the upstream plasma property profiles will make it possible to control the power dispersal on the divertor plate.

PACS numbers: 52.65.Kj, 52.65.Pp, 52.55.Fa
Keywords: KSTAR, High-recycling director operation regine, Edge plasma transport, 2-dimensional fluid simulation

## I. INTRODUCTION

The edge region of the tokamak has a great influence on both plasma confinement in the core region and divertor material protection from the hot core plasma; thus, a number of intensive research activities have been conducted on this region. Most of the critical mechanisms of heat and particle transports take place in this region, and, in turn, successful steady-state operation and device maintenance depend on how the divertor can effectively disperse the plasma power exhausted from the core plasma, control impurity particles, and remove the fuel and fusion by-products (usually helium 'ash'). Therefore, along with the issues of plasma confinement, understanding of divertor physics is one of the most crucial tasks in tokamak research.

The divertor operation regimes are classified in order of increasing Coulomb collisionality [1] by raising the density at a constant input power in experiments. Another way to scan these operation regimes is to increase radiation losses at a constant upstream density so that the target temperature can be lowered. Divertor operations have been tried in two major regimes in accordance with the location of the major volumetric ionization source: *an attached regime* where the target plate temperature is high enough for the ionization front to stay 'attached' to the target, and *a detached regime* where the plate temperature falls to a few electron volts so that the ionization front moves upstream and remains 'detached' from the plate [2]. In the attached regime, the divertor temperature is sufficiently high that friction processes can be neglected in comparison to ionization, and the plasma pressure is kept constant along the field line. The attached regime is further divided into two subregimes based on the ability of the SOL (scrape-off layer) to sustain a significant temperature difference between the upstream and the target: *the linear (sheath-limited)*

*E-mail: kojins@fusma.snu.ac.kr

and *the high-recycling (conduction-limited) regimes.*

Although the detached plasma condition seems to be attractive in terms of divertor heat load and power reduction, the high-recycling divertor operation is often considered to be beneficial in many experiments for some practical reasons [1]. The high-recycling regime is always preferable to the sheath-limited one not only due to the high upstream temperature adjacent to the core plasma, which works to achieve a good confinement, but also due to the low divertor temperature, which reduces the physical sputtering from the plate. On the other hand, a strong detachment condition often leads to the Multifaceted Asymmetric Radiation From the Edge (MARFE) which, in turn, causes the tokamak to reach its density limit and an eventual disruption [3]. The counterbalancing effect against such radiation instability is a thermal conduction capable of redistributing the heat to local radiation spots, which is most apparent in the conduction-limited high-recycling regime. Therefore, tokamak operations close to a transition from the conduction-limited to the detached regimes are sometimes preferable.

Since 1996, the Korea Basic Science Institute (KBSI) has undertaken an independent fusion research program, called Korea Superconducting Tokamak Advanced Research (KSTAR) [4,5]. The conceptual and basic designs of the KSTAR tokamak device have been completed, and the program is currently in its second phase where basic facility construction is the main issue. The KSTAR tokamak device is scheduled to make its first plasma in 2005. In the KSTAR divertor design, attention has been focused on the subjects of reliable power handling, particle control, material choice for divertor plate, and shaping flexibility to accommodate a wide range of plasma operations. According to a simple model that predicts peak heat loads and scales them with the heating power for the KSTAR tokamak designed to have a total input power of 15.5 MW in the baseline operation, the heating power should be lower than 14 MW so as not to exceed the engineering limit of 3.5 MW $\mathrm{m}^{-2}$ for the divertor plate [6]. However, the heating power at the initial stage of the KSTAR operation is not that high; thus, a study of high-recycling operation at a lower heating power should not be ignored. Moreover, this low-power operation will cover some of the baseline operation mode. Hence, it is suggested that this aspect of divertor research is worth investigating through numerical simulations.

In this work, numerical calculations for the KSTAR tokamak are performed to find the operating space for the high-recycling divertor regime in terms of the upstream density and the input power and to investigate various edge plasma characteristics in this divertor operation regime. In the following, a numerical modeling of transport phenomena of the plasma and neutrals in the edge region is summarized to describe the EDGETRAN [7] and NTRAN [8] codes, respectively. Next, the simulation results calculated by using the two codes are discussed by making comparisons with an analytic model and other experimental evidence. The high-recycling characteristics of the temperature difference and the pressure balance between upstream and the divertor are identified, and the scalings of the divertor plasma parameters and the relationship between upstream conditions and divertor power dispersal are discussed. Finally, a summary of this work is presented.

## II. NUMERICAL MODELING

In order to calculate plasma variables, such as ion and electron temperatures and densities, in the SOL, including the upstream position and the divertor region, the numerical simulations in this work use a two-dimensional two-fluid edge plasma transport code, EDGETRAN [7]. The particle, momentum, and energy source terms that appear in the plasma transport equations in the EDGETRAN code, are provided by calculations using a two-dimensional Monte-Carlo neutral transport code, NTRAN [8].

### 1. Two-dimensional Edge Plasma Transport

The moment equations formulated by Braginskii [9] are used to model the plasma transport phenomena in the edge region, and these transport equations are appropriately modified by the assumption of quasineutrality ($n = n_e = n_i$) and negligible electron mass ($m_e \ll m_i$) in a two-fluid plasma. For the equations of continuity,

$$\frac{\partial n}{\partial t} + \nabla \cdot (n\boldsymbol{u_i}) = S_n, \tag{1}$$

$$\nabla \cdot \boldsymbol{J} = 0. \tag{2}$$

For the electron and the ion momentum balance equations,

$$-\nabla p_e + n\left[\nabla\phi - \left(\boldsymbol{u_i} - \frac{\boldsymbol{J}}{ne}\right) \times \boldsymbol{B}\right] + \boldsymbol{R_{ei}} = 0, \tag{3}$$

$$mn\left[\frac{\partial \boldsymbol{u_i}}{\partial t} + (\boldsymbol{u_i} \cdot \nabla)\boldsymbol{u_i}\right] = -\nabla p_i - \nabla \cdot \boldsymbol{\Pi_i} + \boldsymbol{J} \times \boldsymbol{B} + \boldsymbol{S_p} - m\boldsymbol{u_i} S_n. \tag{4}$$

For the electron and the ion energy transport equations,

$$\frac{3}{2}n\frac{\partial T_e}{\partial t} + T_e\nabla\cdot\left(n\boldsymbol{u_i} - \frac{\boldsymbol{J}}{e}\right) + \frac{5}{2}\left(n\boldsymbol{u_i} - \frac{\boldsymbol{J}}{e}\right)\cdot\nabla T_e + \nabla\cdot\boldsymbol{q_e} = -\boldsymbol{J}\cdot\nabla\phi + \boldsymbol{u_i}\cdot(\nabla p_e - \boldsymbol{J}\times\boldsymbol{B}) - Q_{ie} + W_e - \frac{3}{2}T_e S_n, \tag{5}$$

$$\frac{3}{2}n\frac{\partial T_i}{\partial t} + T_i\nabla\cdot(n\boldsymbol{u_i}) + \frac{5}{2}n\boldsymbol{u_i}\cdot\nabla T_i + \boldsymbol{\Pi_i} : \nabla\boldsymbol{u_i} + \nabla\cdot\boldsymbol{q_i}$$
$$= \boldsymbol{u_i}\cdot(\nabla p_i - \boldsymbol{S_p}) + \left(\frac{1}{2}mu_i^2 - \frac{3}{2}T_i\right)S_n + Q_{ie} + W_i, \quad (6)$$

where $n$ is the plasma density, $\boldsymbol{u_i}$ the ion velocity, $\boldsymbol{J}$ the plasma current, and $\phi$ the electrostatic potential. The ion source term $S_n$ due to the ionization of neutral hydrogen and the momentum transfer vector $\boldsymbol{S_p}$ due to recycling neutrals are added to the continuity equation, Eq. (1), and to the ion momentum equation, Eq. (4), respectively. In addition to $Q_{ie}$, which represents the energy exchange between ions and electrons through collisions, $W_e$ and $W_i$ appear in the electron and the ion energy balance equations, respectively. Here, $W_e$ is the electron energy loss due to ionization of recycling neutrals and $W_i$ stands for the ion energy change due to charge exchange with neutrals and the ion energy gain due to the ionization of recycling neutrals. These source terms, $S_n$, $\boldsymbol{S_p}$, $W_e$, and $W_i$, are obtainable from neutral transport calculations. Other implicit terms, such as the mean momentum change $\boldsymbol{R_{ei}}$ of electrons due to collisions with ions, the shear stress $\boldsymbol{\Pi_i}$ for ions, and the heat flux densities $\boldsymbol{q_e}$ and $\boldsymbol{q_i}$ carried by electrons and ions, respectively, have their own expressions containing main plasma variables such as $n$, $\boldsymbol{u_i}$, and $T$, and their derivatives. Their explicit expressions with various transport coefficients are listed in Ref. 10, except for the coefficients along the radial (cross-field) direction, which is assumed to be anomalous in this code. The governing equations, Eqs. (1) to (6), are expanded in an orthogonal coordinate system based on the magnetic flux functions with a toroidal symmetry. The equi-flux lines are adopted as the coordinate in the radial direction ($\psi$), and the other coordinate in the poloidal direction ($\chi$) is created by making it orthogonally intersect the first coordinate.

Figure 1 illustrates a calculated domain (ABCDEF) in the edge region of the KSTAR tokamak, and this domain is schematically simplified in Fig. 2 to give a description of boundary conditions. The net parallel velocity and the derivatives of the plasma density and temperature vanish on the symmetry planes (AB and CD). Heat fluxes to the plate are given at the divertor plate (EF). On the private flux plate (DE) and the first wall (FA), instead of giving fixed values, floating values of $n$, $T_e$, and $T_i$ are first guessed and then successively corrected during the iterations. Boundary conditions on the separatrix line (BC) have been modified to accommodate reasonable physical circumstances, including the properties of the core plasma. A more detailed explanation of them is given in the following subsection.

### 2. Determination of Separatrix Boundary Conditions

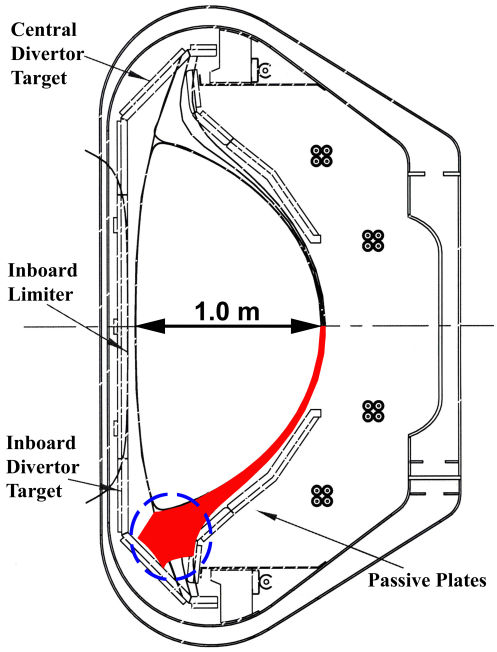


Fig. 1. Calculated domain (shaded area) in the edge region of the KSTAR tokamak.

The parallel fluid velocity along the core boundary [BC in Fig. 2] is set to be zero because this velocity does not affect the divertor target. For finding the plasma density and the temperature, the balance equations for total particles and total energy fluxes are analyzed. The electron and the ion energy fluxes across the core boundary, which are determined by the auxiliary heating power input, are given, respectively, by

$$Q_{e\perp}^{sep} = \frac{5}{2}T_e\Gamma_\perp^{sep} + q_{e\perp}, \quad (7)$$

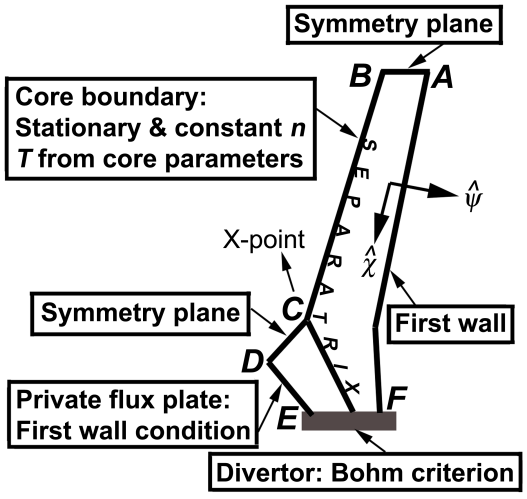


Fig. 2. Schematically simplified geometry of the tokamak edge region with its boundary conditions described.

$$Q_{i\perp}^{sep} = \left(\frac{5}{2}T_i + \frac{m}{2}u_\psi^2\right)\Gamma_\perp^{sep} + q_{i\perp}, \tag{8}$$

where $\Gamma_\perp^{sep}$ is the total particle flux across the core boundary and can be written as

$$\Gamma_\perp^{sep} = nu_\psi - D_\perp(\nabla n)_\psi. \tag{9}$$

The heat fluxes due to the electron and the ion temperature differences are, respectively, given as

$$q_{e\perp} = -\chi_e^\perp(\nabla T_e)_\psi, \tag{10}$$

$$q_{i\perp} = -\chi_i^\perp(\nabla T_i)_\psi. \tag{11}$$

$D_\perp$, $\chi_e^\perp$, and $\chi_i^\perp$ are the prescribed diffusion coefficients of the plasma particles and the thermal energies of electrons and ions , respectively; $u_\psi$ is the ion fluid velocity in the radial direction, and the subscript $\psi$ means the radial component of the accompanying vector.

The total particle flux across the core boundary, $\Gamma_\perp^{sep}$, is related to the particle source in the core plasma, $S_\perp^{core}$, by the relation

$$\Gamma_\perp^{sep} = S_\perp^{core} \times \left(\frac{1/4}{2\pi R_T}\right) \times \left(\frac{1}{1/4 \times 2\pi r_p}\right), \tag{12}$$

where $R_T$ and $r_p$ are the major and the minor radii, respectively, of the tokamak. $S_\perp^{core}$ is evaluated from

$$S_\perp^{core} = \frac{N_{core}}{\tau_p} = \frac{1}{\tau_p}\int_{core} n_{core}dV = \frac{nV_p}{\tau_p}, \tag{13}$$

where $n$ is the volume-averaged plasma density in the core, $V_p$ is the plasma volume. $\tau_p$ is the particle confinement time, which is approximately $2\tau_E$ [11] where $\tau_E$ is the energy confinement time, which is about 140 $msec$ for the KSTAR tokamak [5]. The value of $V_p$ can also be obtained from Ref. 5, and $n$ is calculated from the equation [12]

$$n = n_p + (n_0 - n_p)\frac{1}{\alpha_n^* + 1}, \tag{14}$$

where $n_p$ is the edge (pedestal) density, $\alpha_n^*$ is the value of the density profile exponent (= 1.3), and $n_0$ is the central plasma density. $n_p$ can be given as one of the input parameters for the EDGETRAN code, and $n_0$ is acquired from the Ref. 5 ($\approx 1.0 \times 10^{20}$ m$^{-3}$).

Meanwhile, the value of $n$ calculated from Eq. (14) is assumed to be the line-averaged density in experiments; thus the separatrix density $n_s$ is computed by using the scaling law $\bar{n}_e \approx 3n_s$ [2], where $\bar{n}_e$ is the line-averaged density. The values of $n_s$ obtained in this way in the EDGETRAN code turn out to be valid and reasonable when considering the resultant relation between the edge pedestal density $n_p$ and the separatrix density $n_s$ represented by $n_p \sim 2n_s$ [13]. Once the value of $\Gamma_\perp^{sep}$ is determined from Eqs. (12) $\sim$ (14), Eq. (9) enables us to find the value of $u_\psi$ with $n = n_s$; subsequently, Eqs. (7) and (8) are used to evaluate the values of $T_e$ and $T_i$ at the core boundary.

### 3. Two-dimensional Recycling Neutral Transport

As mentioned in the preceding section, the source terms in the plasma transport equations for the EDGETRAN code should be calculated through analyses of the recycling neutral transport phenomena. The recycling hydrogenic atoms and molecules are produced through neutralization and reflection of incident ions at the divertor plate. They are backscattered and released into the edge plasma from the divertor plate, giving rise to atomic and molecular interactions with background plasma ions and electrons. Molecules are usually dissociated into atoms shortly after they are released, and neutral atoms undergo either a charge-exchange process with plasma ions or an ionization process due to plasma electrons until they strike the wall or the separatrix. The two major atomic interactions of charge exchange with ions, $D^0 + D^+ \rightarrow D^+ + D^0$, and electron-impact ionization, $D^0 + e \rightarrow D^+ + 2e$, are included in the calculation. Other atomic interactions, such as the neutral-neutral and the neutral-ion elastic scattering processes, are not considered due to their negligible contributions. In the charge-exchange process, ions gain momentum and energy as considered in the terms $\boldsymbol{S_p}$ in Eq. (4) and $W_i$ in Eq. (6), respectively. The particle source term $S_n$ in Eq. (1) and the electron energy gain $W_e$ in Eq. (5) are obtained from the electron-impact ionization process.

The NTRAN code is constructed based on the Monte-Carlo numerical scheme in a two-dimensional geometry. If the kind of atomic process is to be determined, not only the neutral density and energy but also the background plasma density and energy on each grid in the calculation domain should be provided, and these values are obtained from the EDGETRAN code. The ion influx to the target is also given by the EDGETRAN code to determine the number of incident ions that become neutrals. Therefore, the edge plasma fluid code and the Monte-Carlo neutral particle code exchange their information on inputs and outputs, by turns, until a certain convergence criterion is met.

## III. CALCULATION RESULTS AND DISCUSSION

### 1. Operation Space for a High-recycling Divertor Regime

The EDGETRAN code has assumed non-ambipolar plasma motions so that it can describe the presence of self-consistent plasma currents. It is capable of calculating the radial and the diamagnetic components of the plasma flow velocity, the electric current vector, the electrostatic potential, and the electric fields, in addition to the main plasma properties, such as the plasma density,

Table 1. Device parameters of the KSTAR tokamak used as the input values in the calculation.

| Parameter | Value |
|---|---|
| Major radius ($R_0$) | 1.8 m |
| Minor radius ($a$) | 0.5 m |
| Elongation ($\kappa$) | 2.0 |
| Triangularity ($\delta$) | 0.8 |
| Toroidal magnetic field ($B_T$) | 3.5 T |
| Plasma current ($I_p$) | 2.0 MA |
| Number of nulls | 2 |
| Energy confinement time ($\tau_E$) | 140 msec |
| Diffusion coefficient ($D$) | 0.5 $m^2/s$ |
| Thermal diffusivity for ions ($\chi_i$) | 1.0 $m^2/s$ |
| Thermal diffusivity for electrons ($\chi_e$) | 1.0 $m^2/s$ |

temperature and parallel flow velocity. In the present numerical work, however, only the main plasma properties are presented since they are of primary importance in analyzing the divertor operation regimes and in comparing their calculated values with those of a simple one-dimensional analytic transport model, referred to as the two-point model [3,14]. Table 1 is a list of some of the device parameters for the KSTAR tokamak that are used as input values for the numerical simulations. In the EDGETRAN code, the particle and the energy transports in the radial direction across the magnetic flux surfaces are assumed to be anomalous. The diffusion coefficient $D$ and the thermal diffusivities $\chi_i$ and $\chi_e$ are given in Table 1 for the KSTAR tokamak based on the previous numerical calculations using the UEDGE code [6] although they can be experimentally obtained from real devices [15].

Table 2 summarizes the values of the heating power and the pulse length for baseline operation phases in the KSTAR program. Since the high-recycling divertor operation regime is a matter of primary concern in the present numerical work, the edge plasma densities are scanned with various constant input heating powers in the KSTAR baseline operation phase so as to find this regime, and some operating windows appearing in the high-recycling regime are listed in Table 3 in terms of the input power supplied by auxiliary heating and the edge (pedestal) plasma density. Some apparent evidence showing these density-power windows in the high-recycling divertor regime will be presented in the next two sections.

## 2. High-recycling Characteristics

Among the plasma characteristics regarded as evidence showing that an SOL plasma is in the high-recycling regime predicted in Table 3, two major features

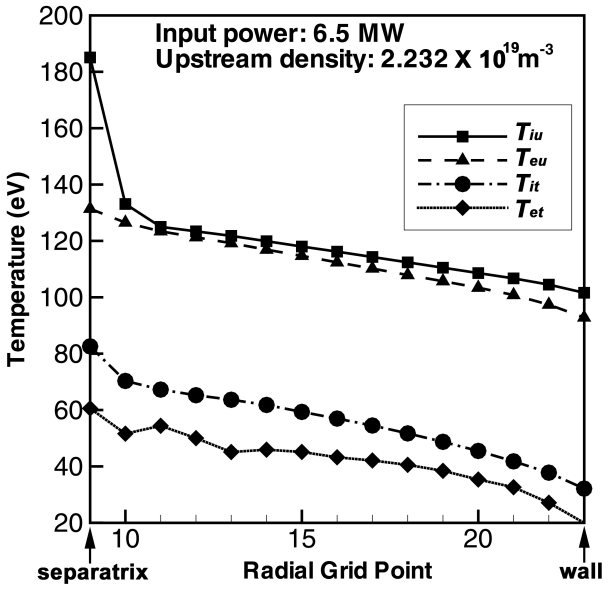


Fig. 3. Radial profiles of the ion and the electron temperatures upstream and at the divertor plate. The upstream density here corresponds to the edge (pedestal) density of 5.1 $\times 10^{19} m^{-3}$.

are discussed, the plasma temperature gradient and pressure conservation along the flux tubes in the SOL ranging from the upstream symmetry plane to the divertor plate.

### *A. Parallel plasma temperature gradient*

Figure 3 describes the radial temperature profiles for ions and electrons at an upstream position and at the divertor plate. The values at the upstream position correspond to those obtained at the outer midplane. As seen in this figure, an apparent temperature difference between the two locations is observed, regardless of species, and the upstream temperature $T_u$ is approximately $2T_t$, where $T_t$ is the temperature at the target plate, for all radial positions, revealing the conduction-limited feature in this regime. Also, the peaked profile of the ion upstream temperature near the separatrix line is sharper than that of electron upstream temperature. This feature has been reported by a number of authors [1,3,16]; the upstream ion temperatures were usually measured to be greater than $2T_e$. Although the upstream ion temperatures are much higher than the upstream electron temperatures near the separatrix, they become thermally equilibrated in the outer region away from the separatrix, as seen in Fig. 3. This is regarded as evidence of a strong parallel conduction to the divertor in the area near the separatrix.

In the divertor target region, ion temperatures are higher than electron temperatures, which implies that the ion energy loss due to charge exchange with neutrals is relatively weak compared to the electron energy loss

Table 2. Heating powers planned for operational phases in the KSTAR program. The power in the parentheses is for start-up.

| Operation Phase | First Plasma | Ohmic Plasma | | Baseline Operation | | |
|---|---|---|---|---|---|---|
| Pulse length (sec) | $\geq 0.1$ | $\leq 10$ | $\leq 10$ | $\leq 20$ | $\leq 20$ | $\leq 20$ |
| NBI (MW) | – | – | – | 8 | 8 | 8 |
| ICRH (MW) | – | – | – | – | 6 | 6 |
| LHCD (MW) | – | – | – | – | – | 1.5 |
| ECH (MW) | (0.5) | (0.5) | 0 | (0.5) | (0.5) | (0.5) |
| Total auxiliary | 0.5 | 0.5 | 0 | 8.0 | 14.0 | 15.5 |
| Heating (MW) | (Start-up) | (Start-up) | | (0.5) | (0.5) | (0.5) |

due to ionization. In other words, the high-recycling feature represents an overwhelming ionization process rather than a charge-exchange process. The temperatures in the target area are considerably higher than 5 eV, a temperature at which the charge-exchange process begins to be significant. Such high temperature at the target plate in the simulation may result from the neglect of the radiative cooling mechanism due to either neutral hydrogens or impurities.

The relative importance of the ionization process near the target can be inferred from Fig. 4 where the temperature profiles of the ions and the electrons along the separatrix line are plotted from the X-point to the target plate. While the ion temperature steadily decreases along the separatrix line, the gradient of the electron temperature becomes steeper near the divertor, which implies that the electron energy loss due to ionization is significant near the divertor target. Since there are no energy sources and sinks along the field line from upstream to the X-point, no temperature changes along the parallel direction are expected in the upstream region above the X-point.

### *B. Pressure conservation*

Ion pressures, as well as electron pressures, are also taken into account in this numerical simulation to evaluate the total plasma pressures, i.e., the sum of the static and the dynamic pressures, upstream and at the divertor plate. Figure 5 shows the total pressure values at the two regions, as well as conservation of the plasma pressure along the flux tubes over almost all radial locations. Figure 6 shows the ratios of the pressure values at the target to those upstream. These ratios are almost unchanged near unity at any operating window of the edge plasma density for the different heating powers given in Table 3. This suggests that the operating windows of the edge density and input power given in Table 3 are in the high-recycling regime. The upstream density in Fig. 6 corresponds to the edge (pedestal) density in Table 3.

Table 3. Operating windows for the heating power and the edge plasma density appearing in the high-recycling divertor regime.

| Auxiliary heating (MW) | Edge density ($10^{19}\mathrm{m}^{-3}$) |
|---|---|
| 4.5 | $2.1 \sim 2.5$ |
| 5.0 | $2.9 \sim 3.3$ |
| 5.5 | $3.7 \sim 4.1$ |
| 6.0 | $4.4 \sim 4.9$ |
| 6.5 | $5.1 \sim 5.7$ |

## 3. Scalings of Upstream and Divertor Plasmas

Some plasma properties at the target and upstream are scaled with an externally specified parameter, i.e., the upstream plasma density; then, the resulting scaling profiles are compared with the scalings obtained using

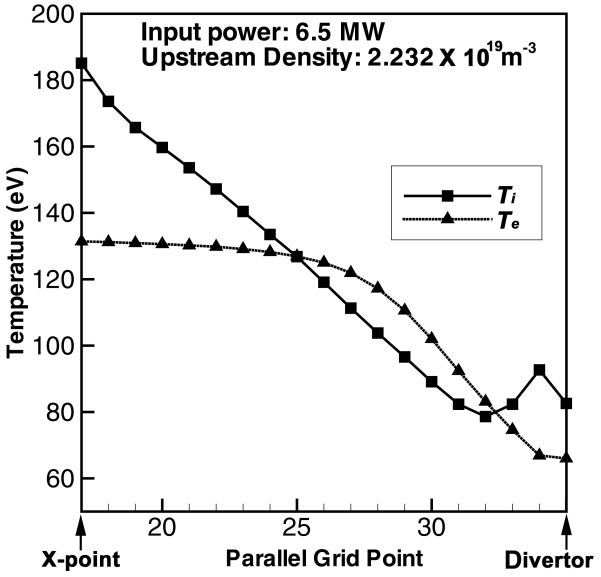


Fig. 4. Parallel profiles of the ion and the electron temperatures along the separatrix line from the X-point to the divertor plate. The upstream density here corresponds to the edge (pedestal) density of 5.1 $\times 10^{19}$ $\mathrm{m}^{-3}$.

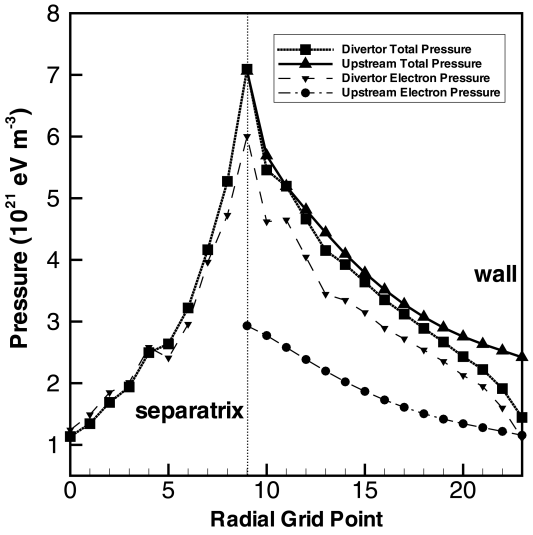


Fig. 5. Radial profiles of the total (ion + electron) and electron pressures upstream and at the divertor plate (input power : 6.5 MW and edge density : $5.1 \times 10^{19}$ m$^{-3}$).

the two-point model [3,16]. According to the two-point model in the high-recycling regime, $T_u$ is independent of the upstream density $n_u$ as long as the input power is constant. However, in practice, $T_u$ with constant input power and no radiation should decrease as $n_u$ increases. For a constant input power of 6.5 MW, an upstream density scanning was done, as presented in Fig. 7(a), to see the variation in the upstream temperature. A linear decrease in the electron and the ion upstream temperatures is observed as the upstream density increases.

The two-point model predicts that $T_t$ will vary as

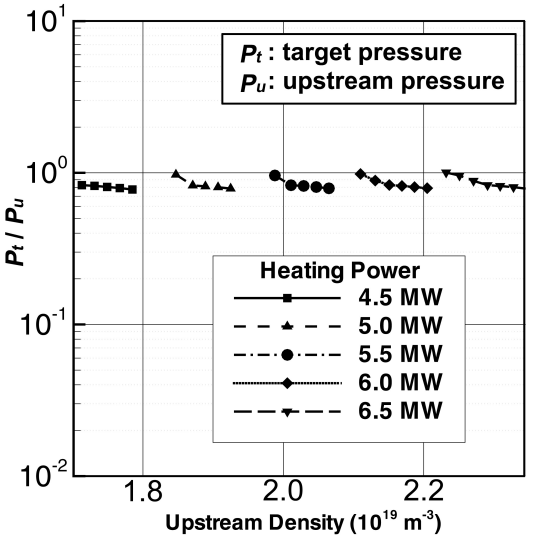


Fig. 6. Ratios of the target pressure to the upstream pressure at the operating windows of the upstream edge density for different input heating powers.

$T_t \propto n_u^{-2}$. The upstream density scanning for constant input power is plotted in Fig. 7(b) and shows that the same relation, $T_t \propto n_u^{-2}$, is valid for ions. In the case of electrons, the $n_u^{-2}$-dependence is rather weak, and the decrease in the electron temperature is seen to stop at a certain upstream density. Such a weak dependence of the electron temperature at the divertor can be explained by the energy loss mechanism of each species. As the upstream density increases, the particle flux to the divertor plate also increases, and this, in turn, increases the number of recycling neutrals. Because of the interactions of these recycling neutrals with plasma particles, the energies of electrons and ions are exhausted, and, thus, their temperatures decrease. A slight decrease in the plasma temperature makes a rather large difference between the charge-exchange and the ionization rate coefficients, the latter decreasing far more rapidly. As the upstream density further increases, this difference becomes more apparent, and electrons lose less energy than ions because of fewer and fewer ionization interactions with the electrons. The existence of a plateau in the electron temperature profile at the target indicates the minimum divertor temperature that the plasma can reach in this operating regime. According to this relation, in the high-recycling divertor regime, the goal of achieving a low plasma temperature near the divertor plate to reduce heat flux and physical sputtering is attainable simply by increasing the (upstream) plasma density.

In Fig. 7(c), the result of density scanning is shown to find the relation between the upstream density $n_u$ and the target density $n_t$. The high-recycling feature of $n_t \propto n_u^3$, which is predicted in the two-point model, is not observed in the present result. The relation between $n_t$ and $n_u$ seen in Fig. 7(c) bears a linear characteristic of $n_t \propto n_u$ as derived in the linear divertor operation regime. Therefore, the plasma conditions in these operating windows are considered not to be in a complete high-recycling regime, but in a transition from the linear to the high-recycling operation regimes [17].

## 4. Upstream Conditions and Divertor Power Dispersal

Figure 8 shows the profiles of the total, the kinetic, and the potential heat fluxes along the field line onto the divertor in the high-recycling regime with increaseing upstream density at a constant power of 6.5 MW. The total heat fluxes, $q_t$, have been calculated by using the equation

$$q_t = n_t c_{St}(\gamma_i T_{it} + \gamma_e T_{et}) + n_t c_{St} \epsilon_{pot}, \qquad (15)$$

where $\gamma_i$ and $\gamma_e$ are the sheath energy transmission coefficients for ions and electrons and are taken to be 3.0 and 5.5, respectively. The previous work in Ref. 7 did not include the potential heat flux, the second term in Eq.

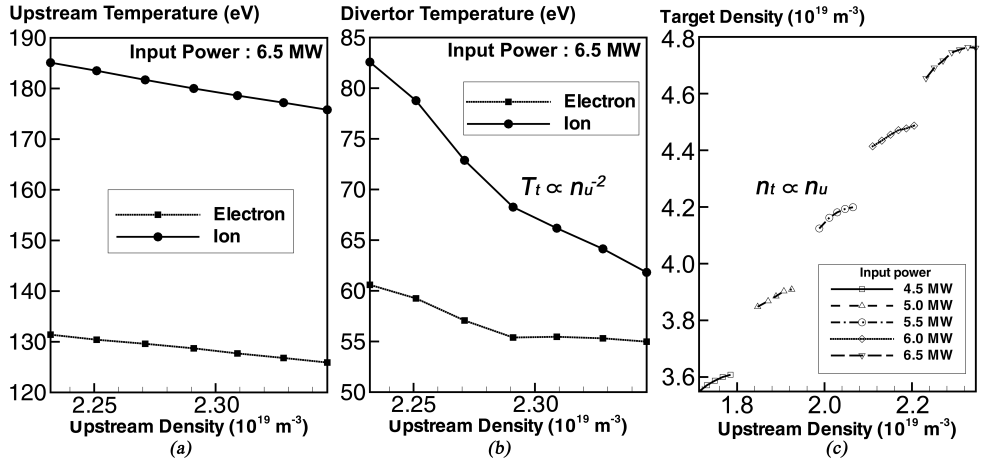


Fig. 7. Scalings of (a) the upstream temperature $T_u$, (b) the divertor temperature $T_t$ and (c) the divertor density $n_t$ with upstream density, $n_u$, scanning for a constant input power of 6.5 MW.

(15). The numerical computation in the present work shows that the contribution of the potential heat fluxes are very small in this high-recycling divertor with high temperatures (see Fig. 8). A small drop in the heat flux with increasing upstream density is also observed in this figure. In evaluating the actual parallel heat fluxes to the divertor, we take into account a correction of a factor of $\sim 0.7$ caused by a tilt angle of 45 degrees between the divertor plate and the field line.

Finally, evidence of the correlation between the upstream plasma conditions and the target power dispersal is seen in Fig. 9 for radial profiles of the upstream ion temperature and the divertor heat flux. The peaked feature near the separatrix, appearing in the target heat flux profile, resembles that in the upstream temperature profile. The power deposition on the plate very close to the separatrix line is nearly coincident with the narrow ion conduction channel determined by the upstream ion temperature profile and the usual contribution of electron heat conduction [3]. Also, in the figure, two power decay lengths exist in the target heat flux profile. Some correlations of the e-folding length of the upstream temperature with that of the divertor heat flux can be found through calculations. This result suggests the possibility of controling the power distribution on the divertor plate by modifying the upstream plasma property profiles. However, one has to be careful not to be misled by the result. It is the upstream profiles, not the absolute values themselves, that affect the heat profiles on the divertor. Therefore, merely increasing the upstream density does not guarantee a full solution to power dispersal on the divertor plate even though it helps to lower the temperatures in this region.

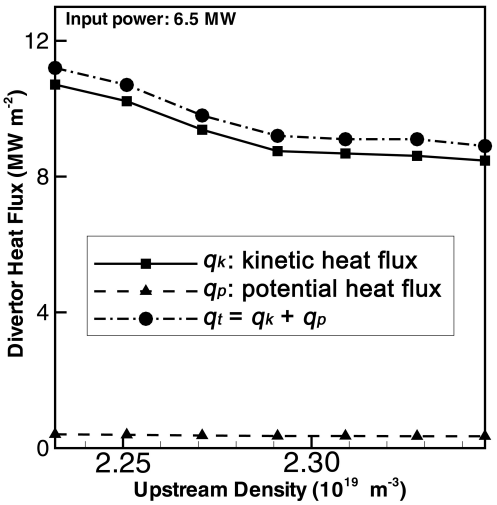


Fig. 8. Dependencies of the total, the kinetic and the potential heat fluxes parallel to the field lines on the upstream density for an input power of 6.5 MW.

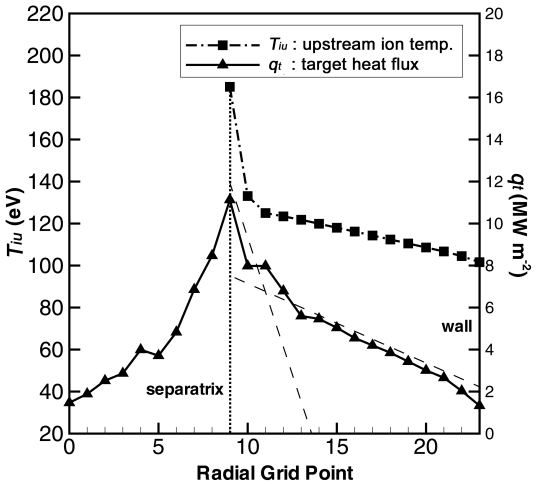


Fig. 9. Dependencies of total, kinetic and potential heat fluxes parallel to the field line on upstream density of an input power of 6.5 MW.

## IV. CONCLUSIONS

The high-recycling characteristics in the upstream and the divertor regions of the KSTAR tokamak have been observed by using two-dimensional edge plasma and recycling neutral transport simulations. For the numerical simulations, the EDGETRAN code for edge plasma transport and the NTRAN code for recycling neutral transport have been used.

A number of runs were conducted in the computing procedures to find the operating windows in terms of the edge (pedestal) density corresponding to the upstream density and the input heating power representing the high-recycling divertor regime. Although the input power ranges were rather lower than expected in the KSTAR standard operation modes, operations with a lower auxiliary heating power can not be ignored because they take a substantial portion in the initial stage of the baseline operation phases in the KSTAR.

The high-recycling divertor operation regimes are featured by both the parallel gradient of the plasma temperature and plasma pressure conservation along the flux tubes. The temperature difference obtained in this numerical simulation agrees well with those obtained in theoretical predictions by other authors [1,3,16], though they are not so remarkable as in the actual tokamak devices which shows $T_u \sim 10T_t$ in the high-recycling regime [17]. The peaked profiles adjacent to the separatrix in the upstream ion temperature and the divertor heat flux indicate that not only the electron conduction but also the narrow ion conduction channel affects the divertor power distribution. Inclusion of the ion pressure in the calculation of the total plasma pressures upstream and at the divertor plate has provided firm evidence of pressure conservation in this regime. The radial temperature profiles for ions and electrons at the divertor region confirm that the ionization process outweighs the momentum transfer process due to charge exchange.

The relationship between the upstream plasma density and temperature is found to be a linear decrease in temperature with increaseing density when radiative processes are not included. The density and the temperature at the divertor can be scaled with the upstream plasma density. For the divertor temperature, the scaling is similar to that of the two-point model prediction while the divertor density scaling has a linear feature ($n_t \propto n_u$) rather than a high-recycling one ($n_t \propto n_u^3$). This gives rise to the hypothesis that the regime under consideration is not in the complete high-recycling regime, but is a transition between the linear and the high-recycling regimes. Temperature scaling also reveals that the target temperature may reach its lowest value in this operation regime. In addition, the similarity between the radial profiles of the upstream temperature and the divertor heat flux suggests the possibility of controlling the divertor heat dispersal by manipulating the upstream plasma profiles, but not the values themselves.

The high-recycling operations have their own advantages of retaining a hot plasma near the core and a pretty cold plasma near the divertor and of securing a density limit that the detached divertor operation can easily reach. Reactor-relevant tokamaks, like ITER, require the plasma temperature near the target plate to be much lower than that reachable in mid-sized tokamaks with moderate input powers. Both the temperature and the density near the divertor should be reduced so that a large input power, for example, of more than 100 MW for ITER, can be tolerated and effectively dispersed at the edge region by appropriate radiative cooling mechanisms, such as the radiative recombination which is significant in detached divertor operation regimes. For this reason, study of detached regimes should be conducted as future work and should take into consideration the radiative process due to either impurities or hydrogenic atoms. Calculations for divertor plasma transport with higher input powers based on various auxiliary heating and current-drive technologies should also be added as a future priority if the KSTAR tokamak is to be a versatile facility capable of operating in the long-pulse and advanced tokamak (AT) operating modes [18].

## REFERENCES


[1] S. K. Erents, Nucl. Fusion **40**, 295 (2000).
[2] ITER Physics Expert Group on Divertor *et al.*, Nucl. Fusion **39**, 2391 (1999).
[3] C. S. Pitcher and P. C. Stangeby, Plasma Phys. Control. Fusion **39**, 779 (1997).
[4] G. S. Lee, Nucl. Fusion **40**, 575 (2000).
[5] M. C. Kyum, T710-AT0-PM0-20000215 / GSLee-E1-Iwd, Controlled Document National Fusion R&D Center (KBSI, 2000).
[6] B. J. Lee, D. Hill, K. H. Im, L. Sevier, J. H. Han and B. J. Braams, Fusion Tech. **37**, 110 (2000).
[7] D. K. Kim, J. M. Ryu, S. H. Hong and K. H. Im, J. Korean Phys. Soc. **31**, S223 (1997).
[8] D. K. Kim, M.S. Thesis, Seoul National University (1995).
[9] S. I. Braginskii, *Reviews of Plasma Physics* (Consultants Bureau, N.Y., 1965), Vol. 1.
[10] J. D. Huba, *NRL Plasma Formulary* (Naval Research Laboratory, Washington DC, 1998).
[11] E. L. Vold, Ph.D. Dissertation, University of California Los Angeles (1989).
[12] *The ARIES-I Tokamak Reactor Study (Final Report)*, UCLA-PPG-1323 (1991).
[13] K. Borrass, Nucl. Fusion **39**, 843 (1999).
[14] J. D. Galambos and Peng Y.-K. M, J. Nucl. Mater. **121**, 205 (1984).
[15] D. H. Chang, K. S. Chung and S. K. Kim, J. Korean Phys. Soc. **37**, 17 (2000).
[16] ITER Physics Basis Editors *et al.*, Nucl. Fusion **39**, 2137 (1999).
[17] C. S. Pitcher, *private communication*, Massachusetts Institute of Technology.
[18] B. G. Hong, J. Korean Phys. Soc. **36**, 90 (2000).